R. & M. No. 2241
(9656)
A.R.C. Technical Report

MINISTRY OF SUPPLY

AERONAUTICAL RESEARCH COUNCIL
REPORTS AND MEMORANDA

An Exact Solution of the Boundary-layer Equations Under Particular Conditions of Porous Surface Suction

By

B. THWAITES, B.A.,
of the Aerodynamics Division, N.P.L.

LONDON: HIS MAJESTY'S STATIONERY OFFICE
Price 1*s.* 3*d.* net

An Exact Solution of the Boundary-layer Equations Under Particular Conditions of Porous Surface Suction

By

B. THWAITES, B.A.,
of the Aerodynamics Division, N.P.L.

Reports and Memoranda No. 2241
May, 1946

Summary.—No hitherto successful attempts except one (by Griffith and Meredith[1]) have been made to provide an exact solution of the boundary-layer equations of motion when there is a continuous normal velocity at the boundary. At the suggestion of Preston[2] a solution is given in this report when this suction velocity is proportional to $x^{-1/2}$, x being the distance along the plate, and there is a constant velocity outside the boundary layer. The solution is merely an extension of the well-known Blasius' solution, and does not contain any new mathematical technique. Being exact, however, it can command a certain interest, since the treatment of the boundary-layer equations with suction through the boundary is very difficult (Thwaites[4]).

The solutions of the differential equation below were obtained on the differential analyser, at Manchester University, at present on loan to the Mathematics Division, N.P.L. Acknowledgements are made to the Analyser Group of this Division for providing these solutions, and in particular to E. C. Lloyd, who was concerned in this particular problem.

Theory.—The equation of flow in the boundary layer is

$$u\frac{\partial u}{\partial x} + v\frac{\partial u}{\partial y} = \nu\frac{\partial^2 u}{\partial y^2} \qquad \ldots \qquad (1)$$

in the usual notation, when the velocity outside the boundary is constant and equal to U. The equation of continuity $\frac{\partial u}{\partial x} + \frac{\partial v}{\partial y} = 0$ allows the use of the stream function ψ for which

$$u = \frac{\partial \psi}{\partial y},\ v = -\frac{\partial \psi}{\partial x}.$$

Using Blasius' well-known transformation,

$$\eta = \tfrac{1}{2}\left(\frac{U}{\nu x}\right)^{1/2} y, \quad \psi = (\nu U x)^{1/2} f,$$

in which f is a function of η only, (1) becomes

$$f''' + ff'' = 0, \qquad \ldots \qquad (2)$$

and u, v are given by

$$u = \tfrac{1}{2}Uf',\ v = \tfrac{1}{2}\left(\frac{U\nu}{x}\right)^{1/2}(\eta f' - f).$$

At the boundary, $\eta = 0$ and $u = 0$, whence $f'(0) = 0$.

The condition at infinity is $u = U$, whence $f'(\infty) = 2$.

Also at the boundary $v = -\tfrac{1}{2}(U\nu/x)^{1/2} f(0)$.

The ordinary Blasius profile is obtained by solving (2) with the conditions

$$f(0) = 0,\ f'(0) = 0,\ f'(\infty) = 2.$$

If however we give $f(0)$ a finite value, we obtain the solution when the velocity of suction is

$$-\tfrac{1}{2}\left(\frac{U\nu}{x}\right)^{1/2} f(0),$$

i.e. proportional to $x^{-1/2}$. The possibility of this and other exact solutions of a similar type was pointed out by Preston[2].

Clearly there is a singularity at the origin and the exact solution will not have much physical significance near that point, but in any case the boundary-layer equations are not good approximations to the full equations of motion near $x = 0$. We can expect, however, that the solution will give a good representation of the physical flow at some distance from the origin.

The solutions of (2) were found on the differential analyser for the boundary conditions $f'(0) = 0$, $f'(\infty) = 2$ and $f(0) = r$, r taking the values 1, 2, 5, 10, 20 in turn. The suction velocity is $v_0 = -\tfrac{1}{2}(U\nu/x)^{1/2} r$, or is given by $-v_0/U = R_x^{-1/2}\,\sigma_1$, R_x being the x Reynolds number, and σ_1 being a number signifying the strength of suction.

The velocity distributions inside the boundary layer for the values $\sigma_1 = 0\cdot5$, 1, $2\cdot5$, 5 and 10 are drawn out in Fig. 1 and are tabulated in Table 1. $\sigma_1 = 0$ corresponds to the ordinary Blasius profile. It will be noticed that as the suction strength increases the velocity profiles become more convex and the width of the boundary layer decreases.

δ^*, the displacement thickness, can be evaluated as follows :—

$$\delta^* = \int_0^\infty \left(1 - \frac{u}{U}\right) dy.$$

Therefore,
$$\tfrac{1}{2}\left(\frac{U}{\nu x}\right)^{1/2} \delta^* = \int_0^\infty [1 - \tfrac{1}{2}f'(\eta)]\, d\eta.$$

To obtain the value of this integral from Table 1, we proceed as follows :—

$$\tfrac{1}{2}\left(\frac{U}{\nu x}\right)^{1/2} \delta^* \simeq \int_0^\delta [1 - \tfrac{1}{2}f'(\eta)]\, d\eta,$$

where δ is the value of η at which $f'(\eta)$ becomes greater than (say) $1\cdot99$. Hence

$$\tfrac{1}{2}\left(\frac{U}{\nu x}\right)^{1/2} \delta^* = \delta - \tfrac{1}{2}[f(\delta) - f(0)],$$

which is immediately evaluated from Table 1 for different values of σ_1. θ, the momentum thickness may be evaluated similarly. Figure 4 shows how δ^* and θ vary with the amount of suction, and it shows that only a small amount of suction is required to produce a large decrease of displacement thickness. On this figure $H = \delta^*/\theta$ is also shown.

It would be interesting to see the configuration of flow and we therefore wish to find ordinates of streamlines. The streamline $\psi = k$ is given by

$$(\nu U x)^{1/2} f(\eta) = k \qquad \ldots \qquad (3)$$

Given k and σ_1 for a certain x, (3) determines $f(\eta)$ and hence η, and hence y. Values of f are given in Table 1, and therefore the ordinates of streamlines are readily evaluable. Figure 2 shows some streamlines near $x = 0$ for $\sigma_1 = 1$, the mass-flow into the surface being equal between each pair of consecutive streamlines. This figure is not without interest, although it probably bears little resemblance to the physical flow, as has been pointed out already. Also on Figure 2 is drawn the displacement thickness δ^*. Figure 3 demonstrates the streamlines over a far greater length of the boundary and this configuration of streamlines is probably close to that in the real flow. The dotted curve in Figure 3 represents the boundary-layer thickness δ, which is defined by $\frac{1}{2}f'(\delta) = u/U = 0{\cdot}995$.

It is suggested that this theory would form the basis of an experiment suitable for a university laboratory. For a porous sheet of material, on each side of which is maintained a constant pressure, the velocity of fluid through it is proportional to $1/t$, t being the thickness of the sheet. Therefore the velocity through a sheet of parabolic form $t = a\sqrt{x}$ is proportional to $x^{-1/2}$, which is the suction velocity distribution considered in this report. The following sketch shows the arrangement which might be employed.

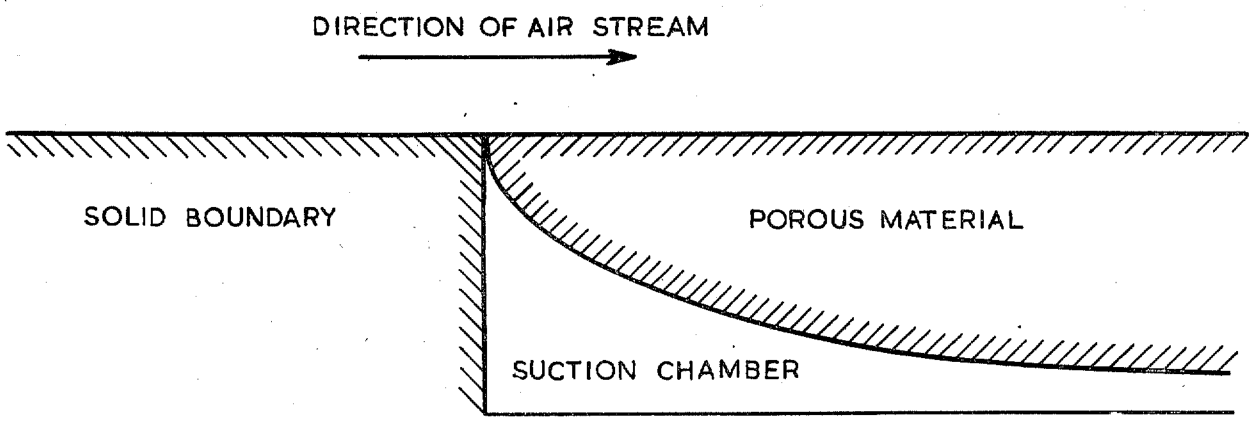

The main feature of this arrangement is the maintenance of a *flat* boundary, thereby avoiding the departure from uniformity of flow if the parabolic sheet were placed in the stream. The growth of a boundary layer along the surface upstream of the porous sheet might be avoided by moving this surface, made of pliable material, round rollers. This arrangement could also be used to test the Tollmien-Schlichting stability theory for different velocity profiles, obtainable by different amounts of suction.

REFERENCES

No.	*Author*	*Title, etc.*
1	Griffith, A. A. and Meredith, F. W.	The Possible Improvement in Aircraft Performance due to the use of Boundary-layer Suction. R.A.E. Report No. E.3501. A.R.C. 2315. March, 1936. (Unpublished.)
2	Preston, J. H.	The Boundary-layer Flow over a Permeable Surface, through which Suction is Applied. R. & M. 2244. February, 1946.
3	Thwaites, B.	On the Flow Past a Flat Plate with Uniform Suction. A.R.C. 9391. February, 1946. (To be published.)
4	Thwaites, B.	Investigations into the Effect of Continuous Suction on Laminar Boundary-layer Flow under Adverse Pressure Gradients. A.R.C. 9555. April, 1946. (To be published.)

TABLE 1

Solutions of $f''' + ff'' = 0$

$f'(0) = 0 \qquad f' \to 2 \text{ as } \eta \to \infty \qquad f(0) = 2\sigma_1$

$\sigma_1 = 0·5$			$\sigma_1 = 1$		$\sigma_1 = 2·5$			$\sigma_1 = 5$			$\sigma_1 = 10$	
η	$f'(\eta)$	$f(\eta)$	$f'(\eta)$	$f(\eta)$	η	$f'(\eta)$	$f(\eta)$	η	$f'(\eta)$	$f(\eta)$	$f'(\eta)$	$f(\eta)$
0	0	1·000	0	2·000	0	0	5·000	0	0	10·000	0	20·000
0·05	0·141	1·004	0·221	2·015	0·025	0·243	5·003	0·00625			0·234	20·001
0·1	0·286	1·014	0·423	2·022	0·05	0·469	5·018	0·0125	0·246	10·001	0·443	20·003
0·2	0·537	1·055	0·779	2·082	0·075	0·650	5·026	0·01875			0·637	20·006
0·3	0·751	1·119	1·05	2·174	0·1	0·813	5·044	0·025	0·457	10·006	0·799	20·011
0·4	0·953	1·204	1·28	2·290	0·15	1·09	5·092	0·0375	0·631	10·013	1·06	20·022
0·5	1·132	1·309	1·46	2·428	0·2	1·31	5·152	0·05	0·795	10·022	1·27	20·037
0·6	1·29	1·430	1·60	2·581	0·25	1·47	5·222	0·0625			1·43	20·054
0·7	1·43	1·566	1·71	2·747	0·3	1·60	5·299	0·075	1·07	10·045	1·56	20·072
0·8	1·54	1·715	1·79	2·922	0·4	1·77	5·468	0·0875			1·65	20·093
0·9	1·64	1·874	1·85	3·105	0·5	1·87	5·561	0·1	1·28	10·074	1·73	20·114
1·0	1·72	2·043	1·90	3·293	0·6	1·93	5·842	0·125			1·84	20·158
1·1	1·79	2·219	1·93	3·484	0·7	1·96	6·037	0·15	1·57	10·146	1·90	20·405
1·2	1·84	2·400	1·95	3·679	0·8	1·98	6·234	0·2	1·74	10·229	1·96	20·302
1·3	1·88	2·584	1·97	3·875	0·9	1·99	6·433	0·25	1·85	10·320	1·98	20·401
1·4	1·91	2·777	1·98	4·073	1·0	1·99	6·632	0·3	1·91	10·414	1·99	20·501
1·5	1·94	2·970	1·99	4·272	1·1	1·99	6·832	0·4	1·97	10·608	2·00	20·701
1·6	1·96	3·165	1·99	4·471	1·2	2·00	7·032	0·5	1·99	10·807		
1·7	1·97	3·362	2·00	4·671				0·6	2·00	11·007		
1·8	1·98	3·559										
1·9	1·99	3·758										
2·0	1·99	3·957										
2·1	1·99	4·157										
2·2	2·00	4·357										

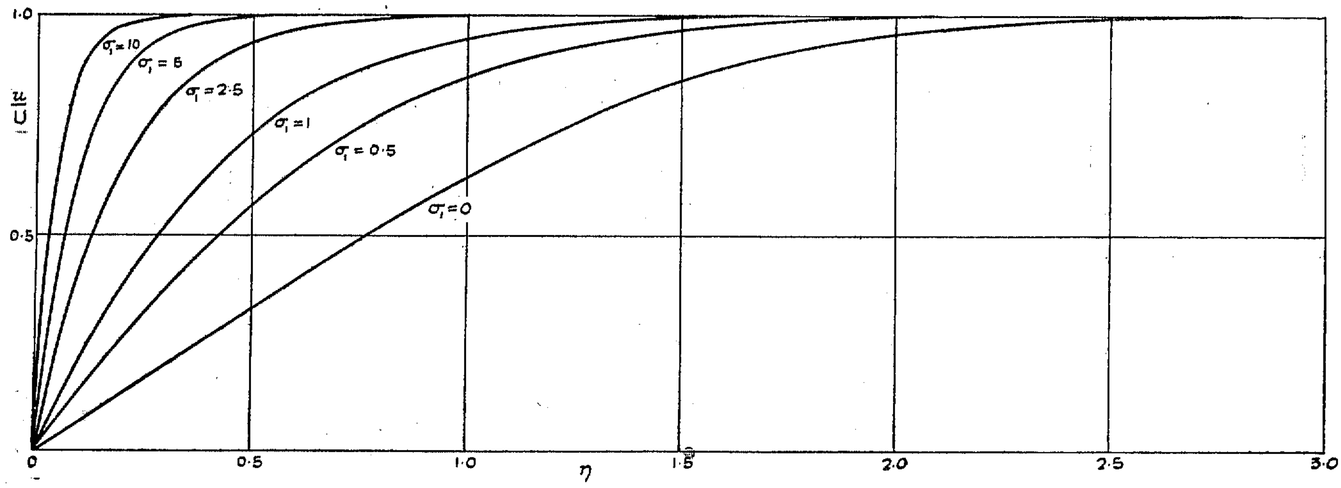
1·0
0·5
u/U
σ₁=10
σ₁=5
σ₁=2·5
σ₁=1
σ₁=0·5
σ₁=0
0
0·5
1·0
1·5
2·0
2·5
3·0
η

FIG. 1.

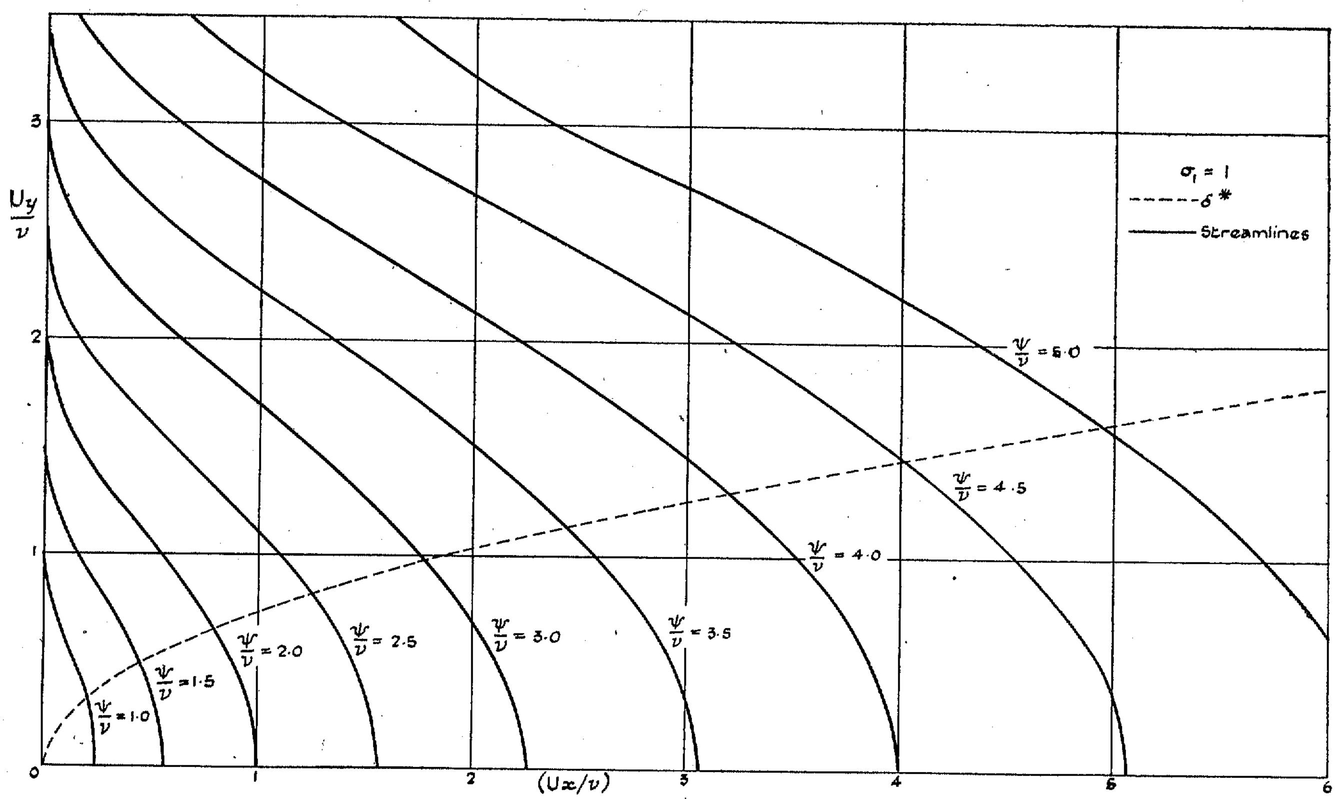
Uy/ν
3
2
1
0
σ₁ = 1
δ*
Streamlines
ψ/ν = 5·0
ψ/ν = 4·5
ψ/ν = 4·0
ψ/ν = 3·5
ψ/ν = 3·0
ψ/ν = 2·5
ψ/ν = 2·0
ψ/ν = 1·5
ψ/ν = 1·0
1
2
(Ux/ν)
3
4
5
6

FIG. 2.

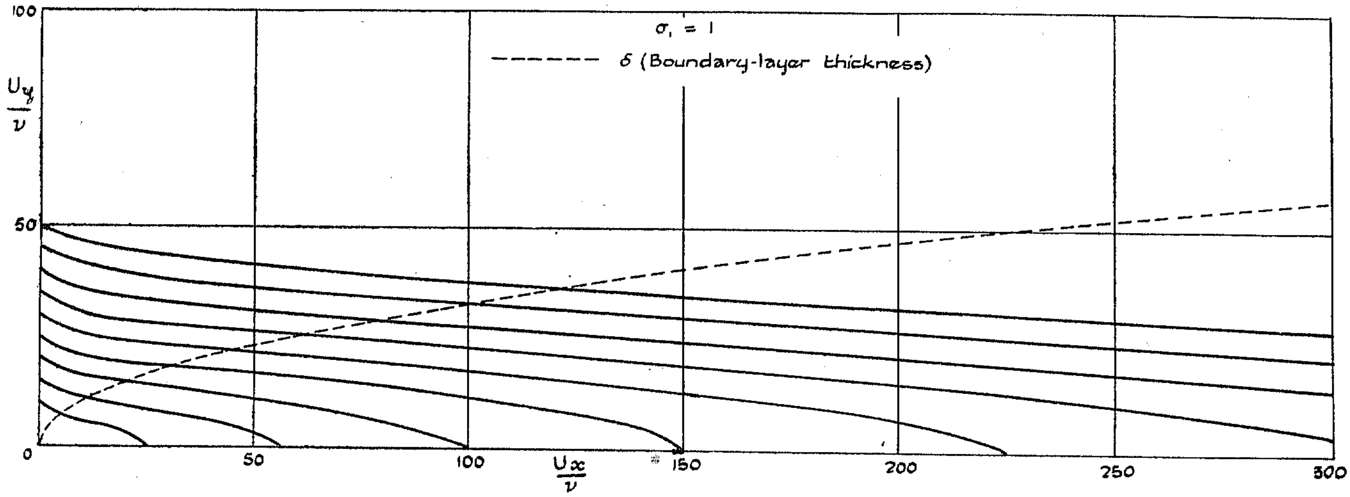

FIG. 3.

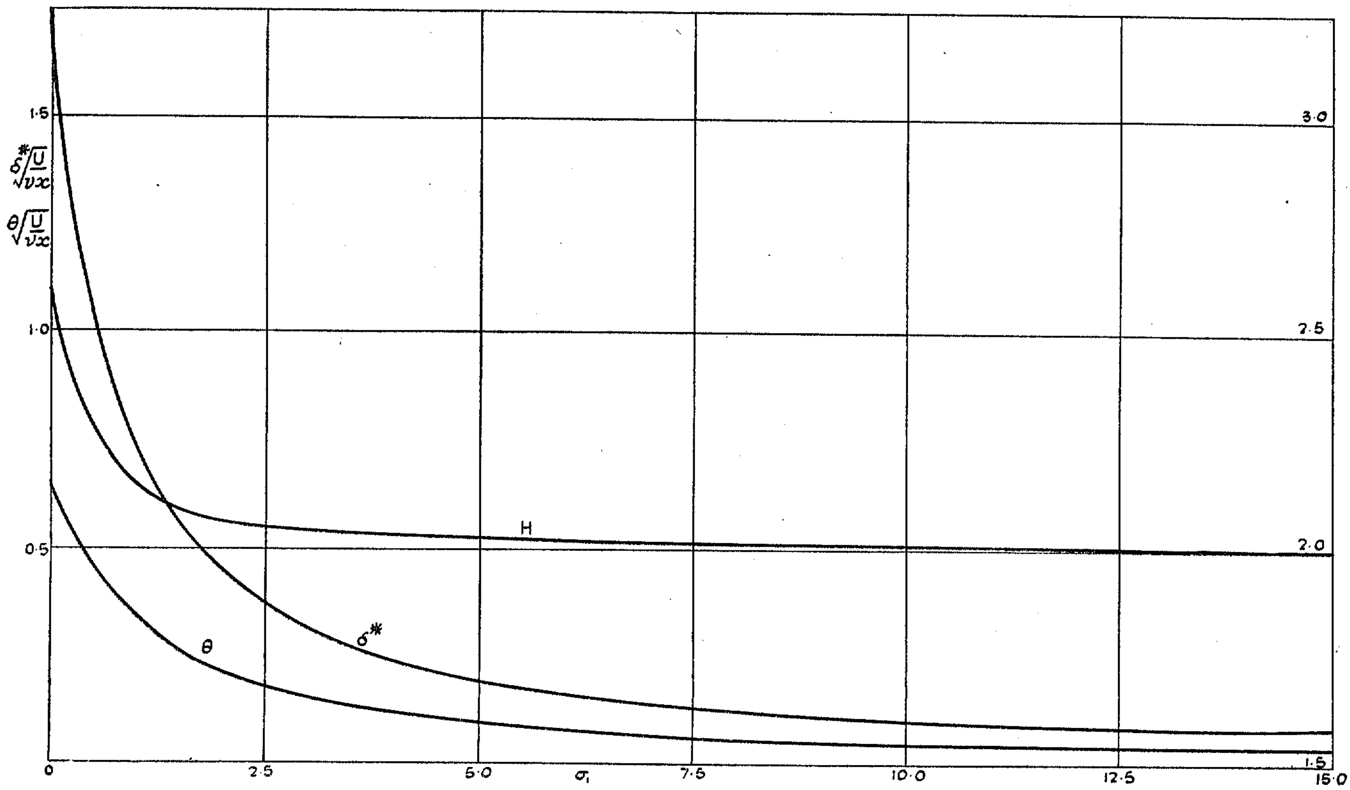

FIG. 4.

(81515) Wt. 11 5/48 Hw.

A Theoretical Discussion of High-lift Aerofoils with Leading-edge Porous Suction

By

B. THWAITES, B.A.
of the Aerodynamics Division, N.P.L.

Reports and Memoranda No. 2242
July, 1946

Summary.—It is shown in this report that by the principle of porous suction high lift coefficients can be obtained on thin aerofoils by the use of surprisingly small amounts of suction. It is more economical to use porous suction than to suck through a slot at or near the leading edge: and it is necessary to realise that in general the principles involved in the two types of suction are rather different. The discussion is restricted to aerofoils with rounded leading edges, since it is difficult to predict theoretically the effect of any type of suction on flow near a sharp edge.

There are given graphs showing estimates of the quantities of air to be sucked on three different typical thin sections to produce any reasonable desired lift coefficient. It seems that to obtain a lift coefficient of 2·0 on a 7 per cent. thick section on a fighter aircraft when landing, a quantity of air of 0·5 cu. ft./sec. per foot span is sufficient, to be sucked over the first 2 per cent. of the chord. Half this quantity of air sucked would suffice for a lift coefficient of 1·5. The design of the leading-edge shape is important but suitable aerofoils have already been designed in Ref. 1.

Introduction and Discussion.—As the speeds at which aeroplanes fly increase, the thickness of their aerofoil sections decrease, and the problem of obtaining a sufficiently high maximum C_L also becomes more acute. Many methods, most of them well known, have been used to produce fairly good max. C_L's on sections of moderate thickness, say 15 per cent., and these have naturally been applied to thinner sections. However, it has now become desirable, if not necessary, to devise rather new methods of obtaining high lift coefficients on thin wings, and furthermore to avoid any large changes of trim that might occur at the same time. In this last respect, too great a use of flaps is undesirable.

The problem therefore reduces to that of extending the lift curve of an aerofoil past the usual stalling point, which implies a prevention of the separation of flow from the nose of an aerofoil at large incidences. There are three principal methods of achieving this: (i) by sucking sufficient quantities of air through the leading edge so that the whole velocity distribution over the aerofoil and especially over its nose is altered in such a way as to delay separation, (ii) by designing the nose of the aerofoil so that at high incidences the usual large adverse velocity gradient is replaced by a discontinuity of velocity at a point where suction is applied to prevent separation, (iii) by using porous suction over the nose, so that the boundary layer is kept thin and in good shape to overcome the adverse velocity gradients. Of these three methods, the second has been considered by Lighthill[2], who also uses a sort of combination of methods (i) and (ii). He derives aerofoils with sharp leading edges. In this report, we shall only consider aerofoils with rounded leading edges, and it will be shown that method (iii) requires far smaller amounts of suction than (ii) to produce high lift coefficients.

1. *Potential Flow Considerations.*—We shall examine the effect of a single suction slot, supposed concentrated at a point on the leading edge, upon the potential flow past an aerofoil. The aerofoil theory notation of Reference 3 will be used, with which the reader is assumed to be familiar.

Suppose that the symmetrical aerofoil has been conformally transformed into the circle $Z = Re^{i\phi}$, so that the point $Z = R$ corresponds to the leading edge. It is easy to verify that the velocity potential due to a sink, of mass-flow m per unit time, at $Z = R$ is

$$w = -\frac{m}{2\pi} 2 \log (Z - R) + \log Z .$$

From this we get

$$u - iv = \frac{dw}{dZ} = -\frac{m}{2\pi}\left(\frac{2}{Z - R} - \frac{1}{Z}\right)$$

and after a little calculation, the velocity at the point $Z = Re^{i\phi}$ is obtained as

$$U = -\frac{m}{2\pi R} \cot \frac{\phi}{2} .$$

Thus the velocity distribution over a symmetrical aerofoil in a stream of velocity $\bar{U}$ is given by

$$\frac{U}{\bar{U}} = F(\theta)\left[\sqrt{1 - \left(\frac{C_L}{a_0}\right)^2} \sin (\theta + \varepsilon) + \frac{C_L}{a_0} \cos (\theta + \varepsilon) + \frac{C_L}{2\pi e^{C_0}} - \frac{m}{2\pi}\frac{4}{c}\frac{1}{\bar{U}} \cot \frac{\theta + \varepsilon}{2}\right], \quad \text{(1)}$$

in which m is the strength of the suction slot at the leading edge. R is approximately equal to $\frac{1}{4}c$.

To find the suction quantity which is necessary to delay the stall up to a certain lift coefficient, we may proceed as follows. Assume that separation of flow does not occur for $m = 0$ at the nose for $C_L = 1$. For any other greater C_L we then find the value of $m/\bar{U}c$, so that the velocity at this C_L has gradients no more severe than those for $C_L = 1$. In this way, we may hope that separation will not occur at this greater C_L and with the amount of suction so determined.

Fig. 1 shows the operation of the method. It can be seen that with a suction velocity given by $m/\bar{U}c = 0{\cdot}0175$ the velocity distribution at $C_L = 1{\cdot}5$ is very similar to that at $C_L = 1{\cdot}0$ with no suction, at which C_L we assume there is no separation.

After this very brief indication of how to estimate the amount of suction required through a single slot, we now proceed to show how much more economical it is to use porous suction.

2. *A Solution of the Boundary-layer Momentum Equation.*—The momentum equation of the boundary layer when there is a velocity $v_0(x)$ normal to the surface is found in Ref. 4 to be

$$UU' (H + 2)\theta + U^2 \frac{d\theta}{dx} = v_0(x) U + \nu \left(\frac{\partial u}{\partial y}\right)_{y=0} . \quad \text{(2)}$$

The equation of motion, taken at $y = 0$ is

$$v_0(x) \left(\frac{\partial u}{\partial y}\right)_{y=} = UU' + \nu \left(\frac{\partial^2 u}{\partial y^2}\right)_{y=0} . \quad \text{(3)}$$

Let us assume $v_0(x)$ is constant, equal to v_0.

Suppose we attempt to maintain a velocity distribution through the boundary layer similar to Blasius' profile. For this,

$$\left.\begin{aligned}\left(\frac{\partial u}{\partial y}\right)_{y=0} &= 0{\cdot}22053 \frac{U}{\theta} , \\ \left(\frac{\partial^2 u}{\partial y^2}\right)_{y=0} &= 0 .\end{aligned}\right\} \quad \text{(4)}$$

Equation (3) gives

$$\left(\frac{\partial u}{\partial y}\right)_{y=0} = \frac{UU'}{v_0},$$

and hence

$$0\cdot22053\,\frac{v_0}{\theta} = U' \quad \ldots \quad (5)$$

The momentum equation (2) becomes

$$0\cdot22053\,\frac{v_0}{\theta}\,U(H+2)\theta + U^2\frac{d}{dx}\left(0\cdot22053\,\frac{v_0}{U'}\right) = v_0U + \frac{UU'}{v_0}\,\nu\,.$$

Therefore

$$-\,0\cdot22053\,Uv_0\,\frac{U''}{(U')^2} = v_0\Big[1 - 0\cdot22053(H+2)\Big] + \nu\,\frac{U'}{v_0}\,. \quad \ldots \quad (6)$$

This is an equation in U which must be solved. We have yet to give a value to H. If we take $H = 2\cdot5345$, the term $v_0\,[1 - 0\cdot22053(H+2)]$ in (6) disappears, thus enabling (6) to be integrated. This is a very reasonable value for H since for Blaisus' profile $H = 2\cdot5911$.

(6) then becomes, after slight re-arrangement,

$$\frac{U''}{(U')^2} + 4\cdot53453\,\frac{\nu}{v_0^{\,2}}\,\frac{U'}{U} = 0\,. \quad \ldots \quad (7)$$

This can be integrated to give

$$-\,\frac{1}{U'} + 4\cdot53453\,\frac{\nu}{v_0^{\,2}}\log\frac{U}{U_0} = 0\,,$$

in which the constant has been adjusted so that $U = U_0$ when $U' = \infty$ (*i.e.* where $\theta = 0$, from (5)).

The equation can be rewritten as

$$-\,1 + 4\cdot53453\,\frac{\nu}{v_0^{\,2}}\,U'\log\frac{U}{U_0} = 0 \quad \ldots \quad (8)$$

and can then be integrated a second time to give

$$\frac{xv_0^{\,2}}{U_0\nu} = 4\cdot53453\left(\frac{U}{U_0}\log\frac{U}{U_0} - \frac{U}{U_0} + 1\right), \quad \ldots \quad (9)$$

in which the constant has been adjusted so that $U = U_0$ when $x = 0$.

The following Table can then be compiled, for U' is found in terms of U from (8) and θ from U' by (5).

$\frac{U}{U_0}$	1	0·9	0·8	0·7	0·6	0·5	0·4	0·35	0·3	0·25	0·2
$\frac{xv_0^{\,2}}{U\nu}$	0	·0236	0·0974	·2285	·4239	·6957	1·0587	1·2813	1·5364	1·8294	2·1680
$-\frac{\theta v_0}{\nu}$	0	·1053	·2231	·3568	·5109	·6931	·9162	1·0499	1·2041	1·3863	1·6094

Fig. 2 demonstrates these results.

The above analysis has appeared before as part of Reference 5.

3. *Application of this Solution to Aerofoils at Large C_L's.*—It will be noticed that the velocity distribution $U(x)/U_0$ of § 2 approximates to that over the nose of an aerofoil at high incidences, and we know how much air must be sucked through the surface to ensure that the boundary-layer profile remains constant (according to the momentum equation, at least).

Suppose now that we know the velocity distribution over the nose of an aerofoil at a high C_L. Fig. 3 shows such distributions for a few C_L's on a typical aerofoil, where x denotes distance along the surface. We must first calculate these distributions in terms of U/U_0, where U_0 is the maximum velocity. The full lines in Fig. 4 show the velocity distributions of Fig. 3 plotted in terms of U/U_0. The point $x/c = 0$ in Fig. 4 now represents, by a slight change of notation, the point of maximum velocity in Fig. 3 for each value of C_L. We must now try to identify these curves with the velocity distribution outside the boundary layer calculated in § 2 and shown in Fig. 2. For this distribution, we notice that the scale of distance along the surface is $xv_0^2/U_0\nu$ and is therefore dependent on the velocity of suction (and the maximum velocity). The curve U/U_0 of Fig. 2 is therefore placed on Fig. 4 with a scale of $xv_0^2/U_0\nu$ adjusted so that the curve fits fairly closely to one of the full-line curves corresponding to a certain C_L. For example, for $C_L = 1 \cdot 0$ if the scale of $xv_0^2/U_0\nu$ is taken as shown, the corresponding dotted curve of U/U_0 approximates to the full-line curve for $C_L = 1 \cdot 0$. It is now possible to find the velocity of suction by comparing the two scales of x/c and $xv_0^2/U_0\nu$; for instance, in this case of $C_L = 1 \cdot 0$, $xv_0^2/U_0\nu = 1 \cdot 0$ when $x/c = 0 \cdot 1$, whence $v_0^2 c/U_0\nu = 10$,

or
$$\frac{v_0}{\bar{U}} = \frac{U_0}{\bar{U}}\sqrt{\frac{10}{R}},$$

in which R is the Reynolds number of flight, and $\bar{U}$ is the flight speed. The velocity of suction has now been determined.

Next, the distance over which suction should be applied must be found. This can be estimated as follows. We assume that the stall does not occur for a certain C_L, say $C_L = 1 \cdot 0$, and that, if the velocity distribution through the boundary layer approximates to Blasius' profile ,velocity gradients such as those for $C_L = 1 \cdot 0$ can thereafter be overcome without separation occurring. From Fig. 3, we see that if, for $C_L = 2 \cdot 0$, suction can maintain Blasius' profile up to $x/c = 0 \cdot 03$, then the flow is unlikely to separate after this point, since the gradients are no more severe than for $C_L = 1 \cdot 0$. Thus for $C_L = 2 \cdot 0$ it is sufficient to use suction for $0 \leqslant x/c \leqslant 0 \cdot 03$. In this way, the extent of suction for any C_L can be estimated.

In Fig. 5, curves of $(v_0/\bar{U})\sqrt{R}$ and x_0/c against C_L are drawn, for the particular aerofoil we have been considering. The total quantity Q of air to be sucked per unit time per unit span is easily found as follows :—

$$Q = x_0 v_0 = \frac{x_0}{c}\frac{v_0}{\bar{U}}\sqrt{R}\left(\frac{c\bar{U}}{\sqrt{R}}\right),$$

$$\frac{Q}{\bar{U}c}\sqrt{R} = \left(\frac{x_0}{c}\right)\left(\frac{v_0}{\bar{U}}\sqrt{R}\right),$$

and a curve of $(Q/\bar{U}c)\sqrt{R}$ against C_L can be drawn as in Fig. 5 from the two previous curves.

4. *The Three Aerofoils and Remarks Thereon.*—(i) H.S.A.VI.—This aerofoil was designed for a very high-speed fighter for which a high max. C_L is desirable. Leading-edge porous suction is likely to be fitted to an experimental aircraft, and calculations were made to determine the amount of air required to be sucked.

The aerofoil is 7 per cent. thick and has a leading-edge radius curvature equal to $0 \cdot 01c$.

Figures 3, 4, 5 pertain to this aerofoil. We assume that, without suction, a C_L of $1 \cdot 0$ can be attained.

(ii) H.S.A. V.—This aerofoil was designed as a possible high-speed aerofoil, in which the velocity distribution at $C_L = 0 \cdot 1$ was such that the magnitude of the maximum velocity is small except for a sharp velocity peak near the nose. Figs. 8 and 6 show the shape of the aerofoil and the velocity distribution over the upper surface at $C_L = 0 \cdot 1$, and also for some high lift coefficients. The considerations which led to its design are that as the Mach number increases, a weak shock wave will appear first near the leading edge, but this will not unduly affect the drag. Eventually, of course, a much stronger shock wave will occur further back when the flow is supersonic over a large part of the surface, but it is conjectured that, in this way, a high critical Mach number is achieved for the thickness of 10 per cent. The behaviour above the critical Mach number, of course, may well be more adverse than usual. However, apart from high-speed characteristics, this aerofoil has an extremely large leading-edge radius of curvature, equal to that of a normal 20 per cent. thick wing. The effect of this small curvature at the nose is strikingly shown in Fig. 6 where it is clear that the velocity gradients at large C_L's are far less severe than on more ordinary aerofoils (*cf.* Fig. 3).

Calculations were made of the amount of suction required on this aerofoil to produce high lift coefficients, and the results are shown in Fig. 7.

(iii) EQH 1260.—Calculations were performed on this aerofoil, since it was intended to fit a porous nose on to an aeroplane which flies with this aerofoil. Fig. 9 shows the results.

(iv) *Remarks.*—Comparing the graphs of $(Q/\bar{U}c)\sqrt{R}$ for each of these three aerofoils, it is clear that the effect of a large leading-edge radius of curvature is considerable. The amount of suction required on EQH 1260 is about five times that for H.S.A. V, and this is a very strong argument for proper leading-edge design.

The advantage of porous suction over a leading-edge slot of the type considered in this report is overwhelmingly plain. For a leading-edge slot, a C_L of $1 \cdot 5$ required $m/\bar{U}c = 0 \cdot 0175$ on an ordinary 10 per cent. thick aerofoil, whereas porous suction will enable this C_L to be attained for a quantity given by $m/\bar{U}c = 0 \cdot 0001$ at a Reynolds number of 9×10^6. Porous suction therefore requires in this case, one two-hundredth of the quantity required for the slot.

Conclusion.—It has been demonstrated that porous suction over the leading edge of an aerofoil is a means of obtaining high lift far more economical than sucking air through a slot with the intention of altering the pressure distribution to delay the stall. Estimates have been made of the amounts of air to be porously sucked through the leading edge to obtain high lift coefficients on three rather different aerofoils : the design of the leading edge is seen to be important.

REFERENCES

No.	*Author*	*Title, etc.*
1	Thwaites, B. ..	On the Design of Aerofoil Sections for High-Speed Aircraft. A.R.C. 9076. October, 1945. (Unpublished.)
2	Lighthill, M. J.	A Theoretical Discussion of Wings with Leading-edge Suction. R. & M. 2162. May, 1945.
3	Goldstein, S. ..	A Theory of Aerofoils of Small Thickness. Part I. Velocity Distributions for Symmetrical Aerofoils. A.R.C. 5804. May, 1942. (To be published.)
4	Thwaites, B. ..	On the Flow past a Flat Plate with Uniform Suction. A.R.C. 9391. February, 1946. (To be published.)
5	Thwaites, B. ..	Investigations into the Effect of Continuous Suction on Laminar Boundary-layer Flow under Adverse Pressure Gradients. A.R.C. 9555. April, 1946. (To be published.)

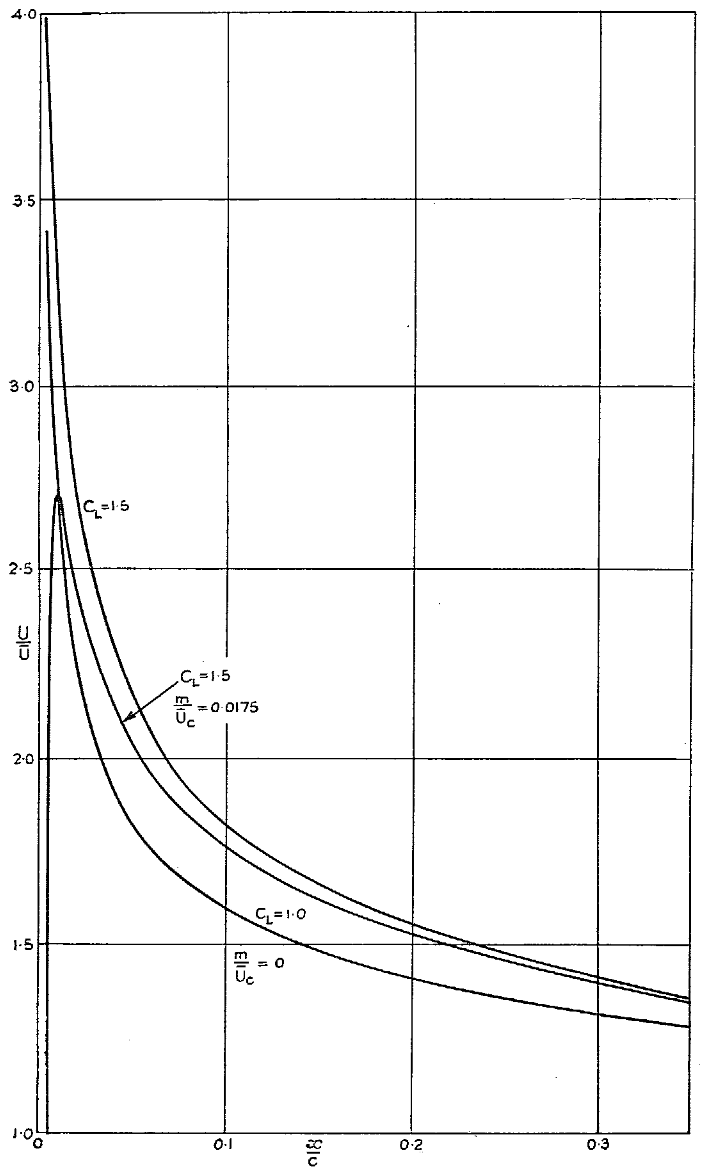
C_L=1·5
C_L=1·5
m/U_c = 0·0175
C_L=1·0
m/U_c = 0
U/c
x/c
1·0
1·5
2·0
2·5
3·0
3·5
4·0
0
0·1
0·2
0·3

FIG. 1

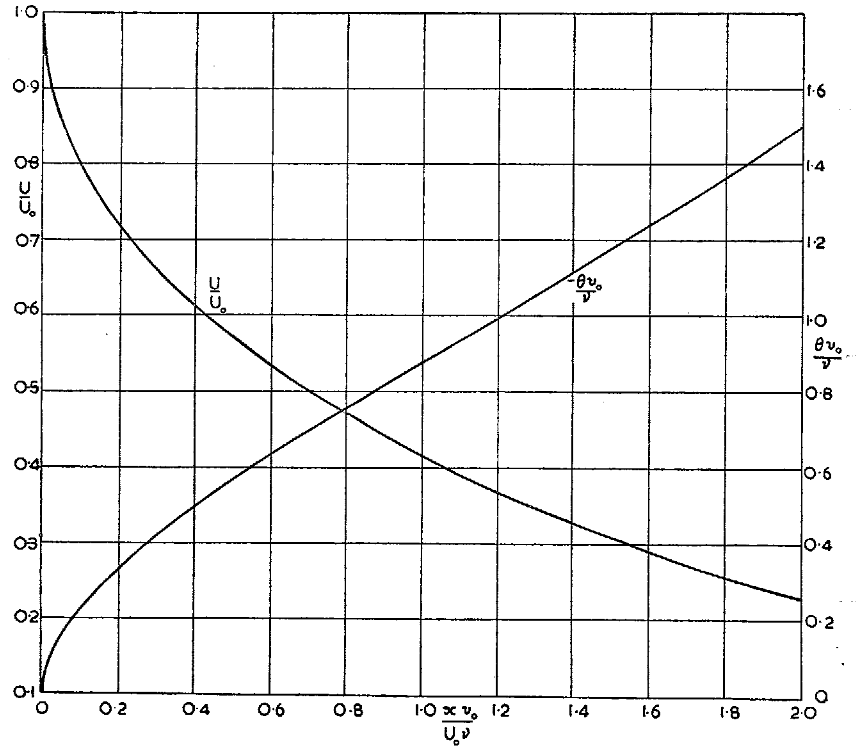
U/U_o
θv_o/v
-θv_o/v
xv_o/U_o v
0·1
0·2
0·3
0·4
0·5
0·6
0·7
0·8
0·9
1·0
0
0·2
0·4
0·6
0·8
1·0
1·2
1·4
1·6
1·8
2·0

FIG. 2

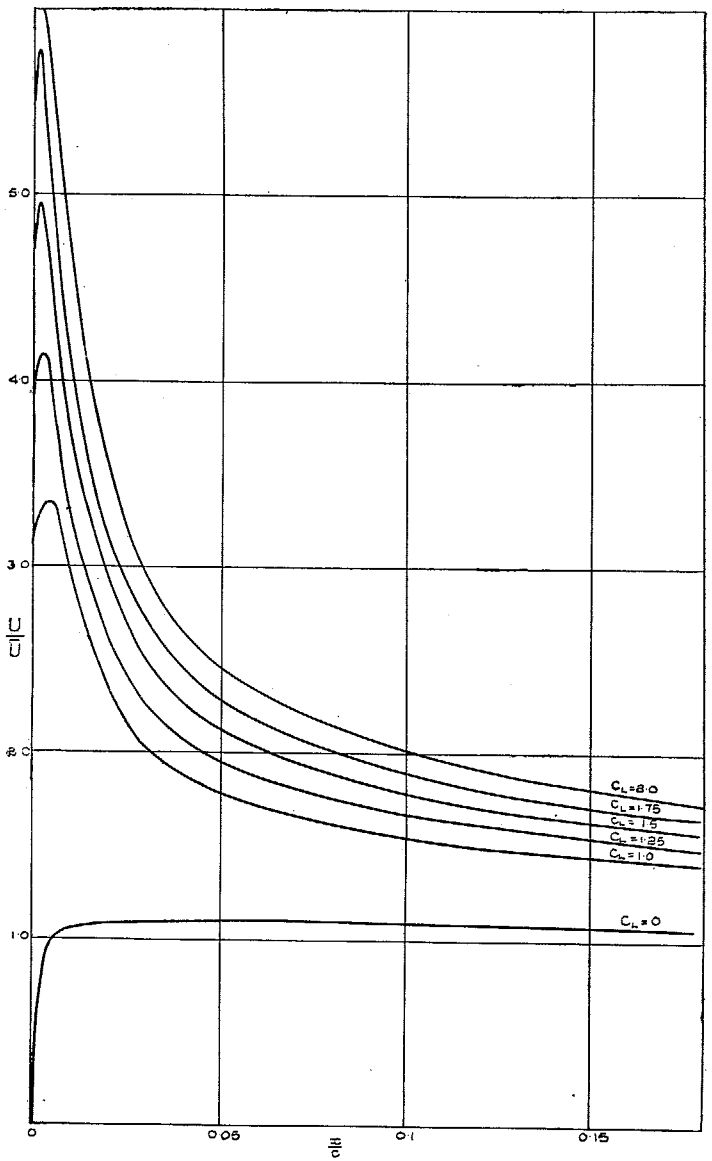
5·0
4·0
3·0
2·0
1·0
U/U
0
0·05
0·1
0·15
x/c
C_L=8·0
C_L=1·75
C_L=1·5
C_L=1·25
C_L=1·0
C_L=0

FIG. 3

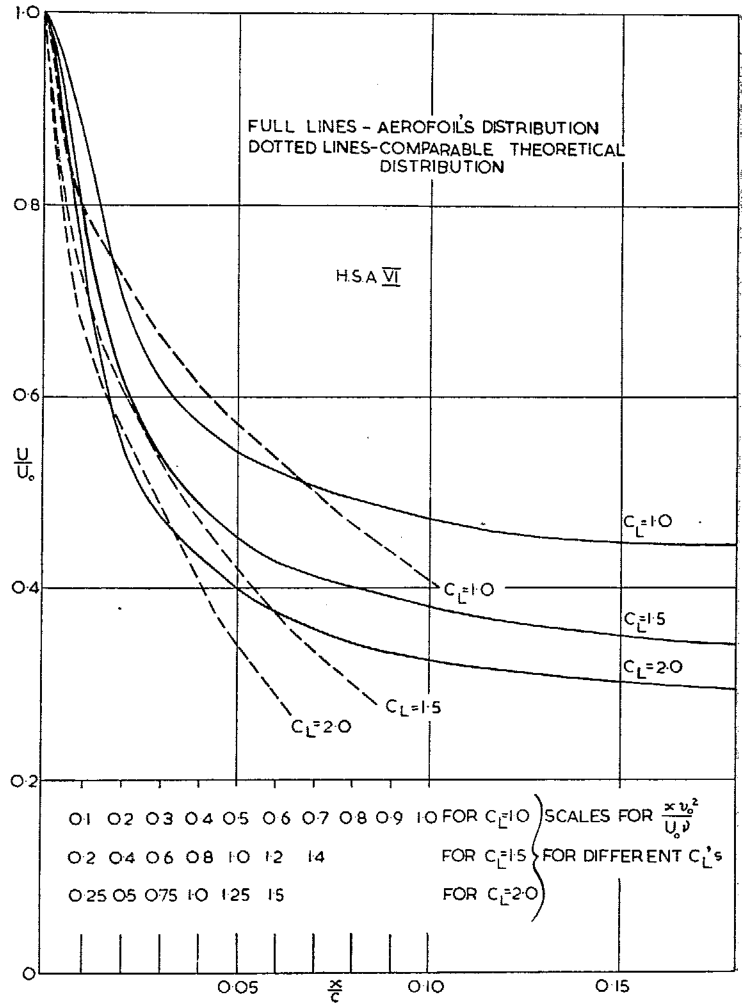
FULL LINES - AEROFOIL'S DISTRIBUTION
DOTTED LINES-COMPARABLE THEORETICAL DISTRIBUTION
H.S.A VI
1·0
0·8
0·6
0·4
0·2
0
U/U₀
C_L=1·0
C_L=1·5
C_L=2·0
C_L=1·0
C_L=1·5
C_L=2·0
0·1 0·2 0·3 0·4 0·5 0·6 0·7 0·8 0·9 1·0 FOR C_L=1·0
0·2 0·4 0·6 0·8 1·0 1·2 1·4 FOR C_L=1·5
0·25 0·5 0·75 1·0 1·25 1·5 FOR C_L=2·0
SCALES FOR xv₀²/U₀ν FOR DIFFERENT C_L's
0·05
0·10
0·15
x/c

FIG. 4

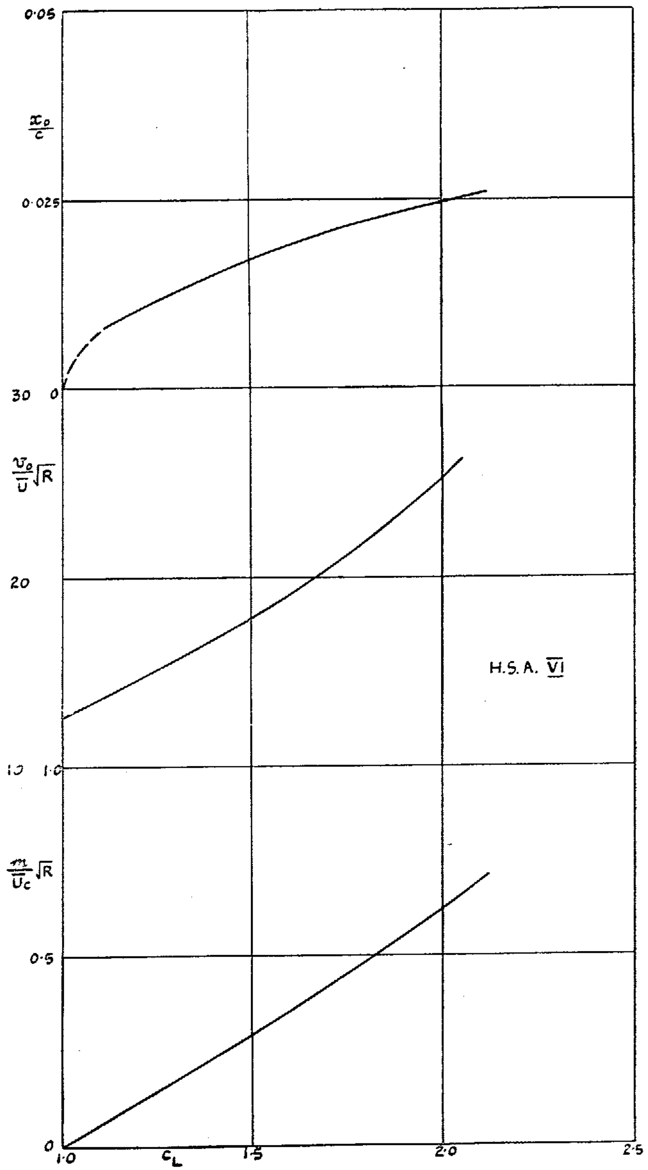

FIG. 5. H.S.A. VI.

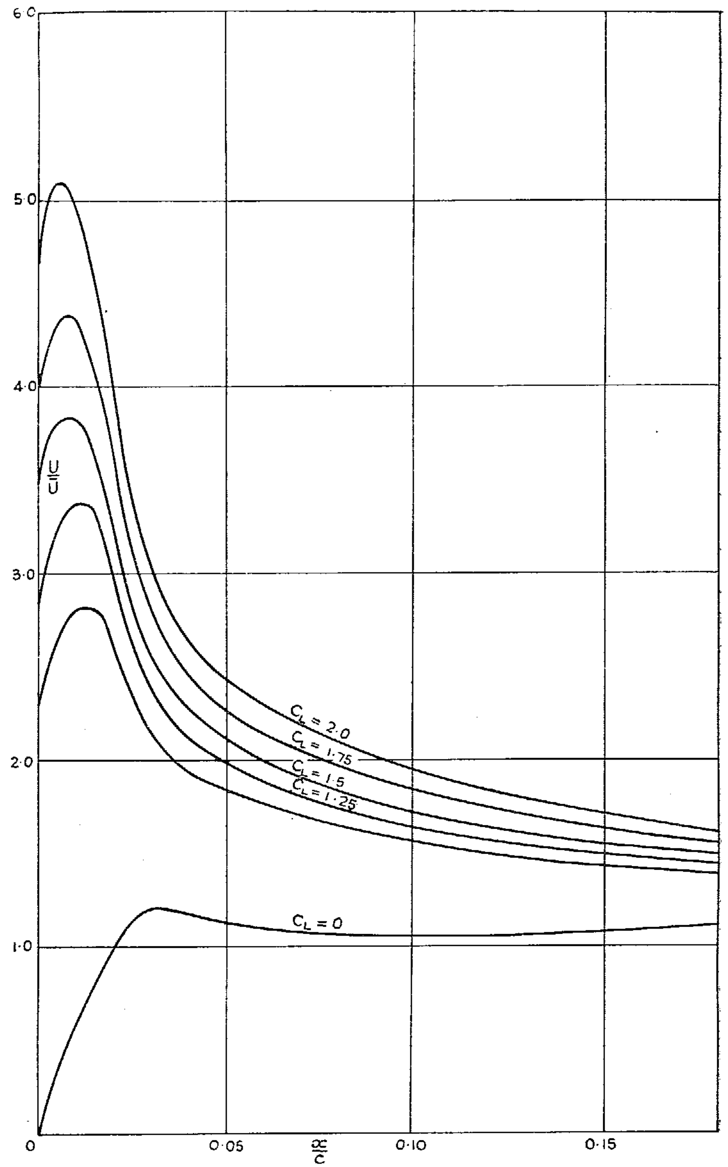

FIG. 6. H.S.A. V.

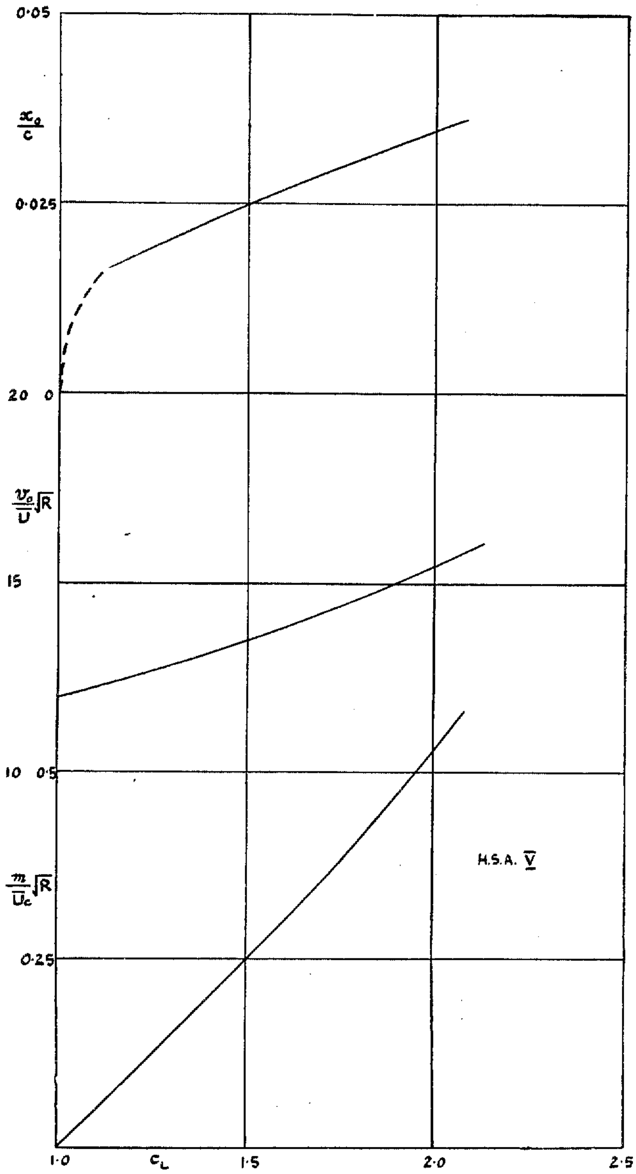

FIG. 7. H.S.A. V.

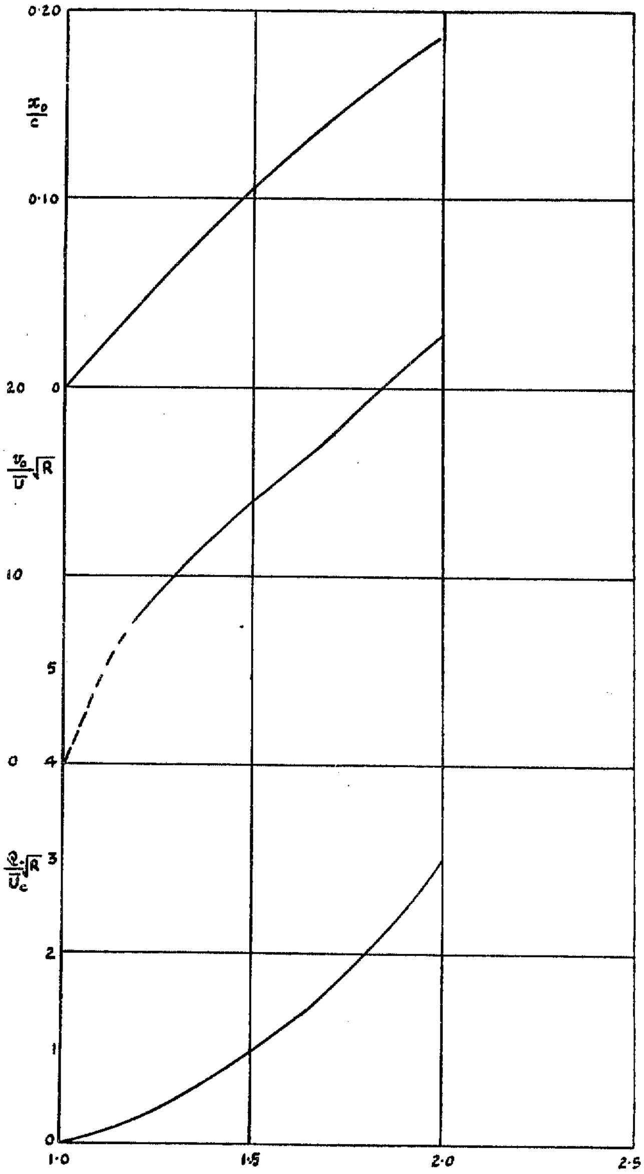

FIG. 9

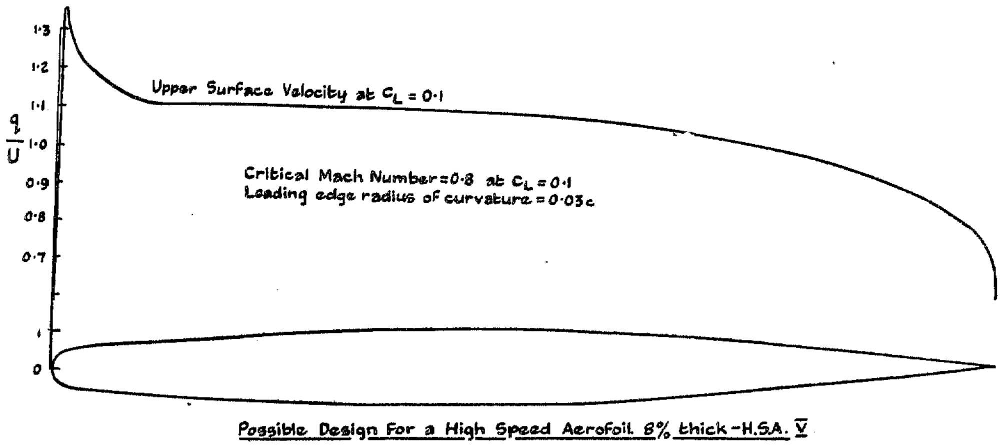

FIG. 8

(82249) Wt. 11 9/49 Hw.

PRINTED IN GREAT BRITAIN

R. & M. No. 2242
(9809)
A.R.C. Technical Report

Publications of the Aeronautical Research Committee

TECHNICAL REPORTS OF THE AERONAUTICAL RESEARCH COMMITTEE—

1934–35 Vol. I. Aerodynamics. 40*s*. (40*s*. 8*d*.)
Vol. II. Seaplanes, Structures, Engines, Materials, etc. 40*s*. (40*s*. 8*d*.)

1935–36 Vol. I. Aerodynamics. 30*s*. (30*s*. 7*d*.)
Vol. II. Structures, Flutter, Engines, Seaplanes, etc. 30*s*. (30*s*. 7*d*.)

1936 Vol. I. Aerodynamics General, Performance, Airscrews, Flutter and Spinning. 40*s*. (40*s*. 9*d*.)
Vol. II. Stability and Control, Structures, Seaplanes, Engines, etc. 50*s*. (50*s*. 10*d*.)

1937 Vol. I. Aerodynamics General, Performance, Airscrews, Flutter and Spinning. 40*s*. (40*s*. 9*d*.)
Vol. II. Stability and Control, Structures, Seaplanes, Engines, etc. 60*s*. (61*s*.)

1938 Vol. I. Aerodynamics General, Performance, Airscrews, 50*s*. (51*s*.)
Vol. II. Stability and Control, Flutter, Structures, Seaplanes, Wind Tunnels, Materials. 30*s*. (30*s*. 9*d*.)

ANNUAL REPORTS OF THE AERONAUTICAL RESEARCH COMMITTEE—

1933–34	1*s*. 6*d*. (1*s*. 8*d*.)
1934–35	1*s*. 6*d*. (1*s*. 8*d*.)
April 1, 1935 to December 31, 1936.	4*s*. (4*s*. 4*d*.)
1937	2*s*. (2*s*. 2*d*.)
1938	1*s*. 6*d*. (1*s*. 8*d*.)

INDEXES TO THE TECHNICAL REPORTS OF THE ADVISORY COMMITTEE ON AERONAUTICS—

December 1, 1936 — June 30, 1939.	R. & M. No. 1850.	1*s*. 3*d*. (1*s*. 5*d*.)
July 1, 1939 — June 30, 1945.	R. & M. No. 1950.	1*s*. (1*s*. 2*d*.)
July 1, 1945 — June 30, 1946.	R. & M. No. 2050.	1*s*. (1*s*. 1*d*.)
July 1, 1946 — December 31, 1946.	R. & M. No. 2150.	1*s*. 3*d*. (1*s*. 4*d*.)
January 1, 1947 — June 30, 1947.	R. & M. No. 2250.	1*s*. 3*d*. (1*s*. 4*d*.)

Prices in brackets include postage.

Obtainable from

His Majesty's Stationery Office

London W.C.2 : York House, Kingsway
[Post Orders—P.O. Box No. 569, London, S.E.1.]

Edinburgh 2 : 13A Castle Street
Birmingham 3 : 2 Edmund Street
Bristol 1 : Tower Lane
Manchester 2 : 39 King Street
Cardiff : 1 St. Andrew's Crescent
Belfast : 80 Chichester Street

or through any bookseller.

S.O. Code No. 23-2242